Environmental Research 212 (2022) 113234

Contents lists available at ScienceDirect

Environmental Research

journal homepage: www.elsevier.com/locate/envres

Spatial dynamics of active microeukaryotes along a latitudinal gradient: Diversity, assembly process, and co-occurrence relationships

Dapeng Xu [a,b,*], Hejun Kong [a,b], Eun-Jin Yang [c], Ying Wang [a,b], Xinran Li [a,b], Ping Sun [d,e,**], Nianzhi Jiao [a,b], Youngju Lee [c], Jinyoung Jung [c], Kyoung-Ho Cho [c]

[a] State Key Laboratory of Marine Environmental Science, Institute of Marine Microbes and Ecospheres, College of Ocean and Earth Sciences, Xiamen University, Xiamen, China
[b] Fujian Key Laboratory of Marine Carbon Sequestration, Xiamen University, Xiamen, China
[c] Division of Polar Ocean Science, Korea Polar Research Institute, Incheon, South Korea
[d] Key Laboratory of the Ministry of Education for Coastal and Wetland Ecosystem, College of the Environment and Ecology, Xiamen University, Xiamen, 361102, China
[e] Fujian Provincial Key Laboratory for Coastal Ecology and Environmental Studies, Xiamen University, Xiamen 361102, China

ARTICLE INFO

Keywords:
SSU rRNA
Northwest Pacific ocean
Arctic
Protist
Latitudinal diversity gradient (LDG)

ABSTRACT

Recent global warming is profoundly and increasingly influencing the Arctic ecosystem. Understanding how microeukaryote communities respond to changes in the Arctic Ocean is crucial for understanding their roles in the biogeochemical cycles of nutrients and elements. Between July 22 and August 19, 2016, during cruise ARA07, seawater samples were collected along a latitudinal transect extending from the East Sea of Korea to the central Arctic Ocean. Environmental RNA was extracted and the V4 hypervariable regions of the reverse transcribed SSU rRNA were amplified. The sequences generated by high throughput sequencing were clustered into zero-radius OTUs (ZOTUs), and the taxonomic identities of each ZOTU were assigned using SINTAX against the PR2 database. Thus, the diversity, community composition, and co-occurrence networks of size fractionated microeukaryotes were revealed. The present study found: 1) the alpha diversity of pico- and nano-sized microeukaryotes showed a latitudinal diversity gradient; 2) three distinct communities were identified, *i.e.*, the Leg-A, Leg-B surface, and Leg-B subsurface chlorophyll *a* maximum (SCM) groups; 3) distinct network structure and composition were found in the three groups; and 4) water temperature was identified as the primary factor driving both the alpha and beta diversities of microeukaryotes. This study conducted a comprehensive and systematic survey of active microeukaryotes along a latitudinal gradient, elucidated the diversity, community composition, co-occurrence relationships, and community assembly processes among major microeukaryote assemblages, and will help shed more light on our understanding of the responses of microeukaryote communities to the changing Arctic Ocean.

1. Introduction

By transforming energy and chemical substrates in a multitude of metabolic processes, marine microorganisms underpin ocean food webs and drive global biogeochemical cycles. (Field et al., 1998; Pomeroy et al., 2007). Among the highly diverse marine microorganisms, most microeukaryotes (single-celled eukaryotes, protists) are microscopic. However, these assemblages exhibit a wide range of morphologies, behaviors, and nutritional modes, including phototrophy, heterotrophy, and mixotrophy, and can perform free-living, symbiont, or parasitic lifestyles (Caron et al., 2012). They form complex ecological networks (Azam et al., 2007; Lima-Mendez et al., 2015) and initiate and govern major biogeochemical cycles on both local and global scales (Field et al., 1998; Falkowski et al., 2008). The traditional approach of microscopy observation has been used to assess microeukaryote diversity by comparing their morphological features (Sournia et al., 1991; Simon et al., 2009), which may largely underestimate the actual extent of their diversity because some pico/nano-sized or parasitic groups are small and lack sufficient morphological traits for accurate separation. In the past several decades, molecular surveys based on the sequencing of

* Corresponding author. State Key Laboratory of Marine Environmental Science, Xiamen University, Xiamen, 361002, China.
** Corresponding author. Fujian Provincial Key Laboratory for Coastal Ecology and Environmental Studies, Xiamen University, Xiamen 361102, China.
E-mail addresses: dapengxu@xmu.edu.cn (D. Xu), psun@xmu.edu.cn (P. Sun).

https://doi.org/10.1016/j.envres.2022.113234
Received 29 June 2021; Received in revised form 24 March 2022; Accepted 28 March 2022
Available online 4 April 2022

marker genes, such as the SSU rRNA gene, have uncovered massive undescribed diversity (Mittelbach et al., 2010; Toseland et al., 2013; Giner et al., 2020). Thus, sequencing approaches, particularly high throughput sequencing (HTS), have been shown to be effective tools for characterizing the biodiversity and biogeography of microbial assemblages, including microeukaryotes, in diverse environments and revealing the environmental driving mechanisms.

Despite recent advances in the biodiversity studies of microeukaryotes, some fundamental topics remain disputed, including, for example, the latitude diversity gradient of protists (LDG). The LDG is one of the most remarkable patterns in nature, occurring in both marine and terrestrial organisms. The general LDG pattern is that alpha diversity decreases as latitude increases. Despite the fact that numerous studies have been conducted on the LDG for a variety of microorganisms, including viruses, bacteria, diatoms, and copepods, no consensus has been reached (Woodd-Walker et al., 2002; Hillebrand, 2004; Fuhrman et al., 2008; Milici et al., 2016; Gregory et al., 2019; Righetti et al., 2019). For example, even the two most recent studies on the LDG of protists produced insistent results. Based on the Tara Ocean global expeditions, Ibarbalz et al. (2019) found a decline in diversity for most planktonic groups, including microeukaryotes, toward the poles. While based on samples collected along a ~15,400-km Pacific Ocean transect, Moss et al. (2020) concluded that Eukarya communities lacked LDG.

Most studies on the biodiversity of microeukaryotes to date have relied on environmental DNA extracts (López-García et al., 2001; Stoeck et al., 2003; Massana et al., 2004; de Vargas et al., 2015; Santoferrara et al., 2016; Ibarbalz et al., 2019; Moss et al., 2020; Zhao et al., 2021). Few have used RNA-based sequencing (Stoeck et al., 2007; Not et al., 2009; Massana et al., 2015; Logares et al., 2014; Hu et al., 2016; Xu et al., 2017, 2018a; Sun et al., 2019, 2020, 2021; Giner et al., 2020; Li et al., 2021). The former was proposed to reveal the total community because environmental DNA could contain nucleic acids from living, dormant, or dead microbial cells, as well as extracellular free DNA (Josephson et al., 1993; Dell'Anno and Danovaro, 2005), whereas the latter was proposed to contain only active members due to the rapid degradation of extracellular RNA molecules (Karl and Bailiff, 1989). Additionally, introns in several key taxonomic groups of diatoms, such as *Chaetoceros*, can render the V4 regions of the SSU rRNA gene too lengthy to sequence using HTS, resulting in the under- or non-representation of some abundant and ecologically significant species when using DNA (Gaonkar et al., 2018, 2020). When the rRNA gene is transcribed into rRNA, the introns are deleted, and so these species can be detected using RNA sequencing rather than DNA sequencing. Most previous studies addressing the LDG of microeukaryotes used SSU rRNA gene sequencing (Fuhrman et al., 2008; Xia et al., 2019; Ibarbalz et al., 2019; Moss et al., 2020). The diversity and community composition of active microeukaryotes in response to the latitudinal gradient remain to be further explored.

Climate change scenarios predict an overall increase in sea surface temperature with substantial impacts on the Arctic Ocean (Ibarbalz et al., 2019; Pachauri et al., 2014). Since the mid-20th century, Arctic air temperatures have risen twice as fast as the global average (~0.7 °C) (Screen and Simmonds, 2010; Stocker et al., 2013). Changes in ocean temperature have the potential to alter plankton diversity, composition, and distribution by affecting their metabolic rates and growth (Thomas et al., 2012; Toseland et al., 2013), the nutrients available to phytoplankton/bacteria, and further higher trophic level organisms in the food webs (Bopp et al., 2013). According to the model study, the most dramatic changes in diversity across most marine planktonic groups are expected to occur in the Arctic Ocean, with a ca. 50% increase in the diversity of non-parasitic protists (Ibarbalz et al., 2019). It is widely established that changes in the taxonomic composition of planktonic communities have substantial impacts on key ecosystem activities such as primary and secondary production, carbon and nutrient cycling, and further ecosystem services (Levinsen and Nielsen, 2002; Beaugrand et al., 2015; Hutchins and Fu, 2017; Brun et al., 2019). Thus, establishing a baseline and conducting continuous surveys of the diversity and community dynamics of Arctic microeukaryotes are critical for inferring the influence of Arctic microorganisms under the global warming scenario. Over the past two decades, environmental sequencing-based techniques have enabled a rapid survey of marine microeukaryotes. Due to sampling problems, studies on Arctic microeukaryotes, particularly those employing environmental RNA-based sequencing, have been sparse in comparison to other marine regimes (Marquardt et al., 2016; Stecher et al., 2016; Comeau et al., 2019; Kalenitchenko et al., 2019; Xu et al., 2020; Liu et al., 2021; Sun et al., 2022). Furthermore, most studies conducted in the Arctic Ocean have focused on the taxonomic diversity of microeukaryotes, leaving functional composition and co-occurrence network analysis largely restricted.

In the present study, we used SSU rRNA-based HTS to evaluate the latitudinal distribution patterns of size-fractionated microeukaryote plankton communities and network analysis to examine the relationships among key microeukaryote taxonomic and functional groups. Our main objectives were to (1) validate the LDG of size-fractionated active microeukaryotes; (2) uncover the co-occurrence patterns of major microeukaryote assemblages, and (3) reveal changes in the community assembly process. Taken together, our work will provide additional insight into the latitudinal patterns of active microeukaryotes and improve our understanding of their co-occurrence relationships in variable environments, with a particular emphasis on the Arctic Ocean under the global warming scenario.

2. Materials and methods

2.1. Sample collection

Thirty-four stations along a latitudinal transect extending from the East Sea of Korea (the Sea of Japan) (A1-A4), the northwestern Pacific Ocean (A7-A15), the Bering Sea (A16-A22), and the Arctic Ocean (B1–B31) were sampled onboard *IBRV ARAON* between July 22 and August 19, 2016, as part of the ARA07 Expedition (Fig. 1, Table S1). Stations labeled with "A" were sampled during Leg-A and stations

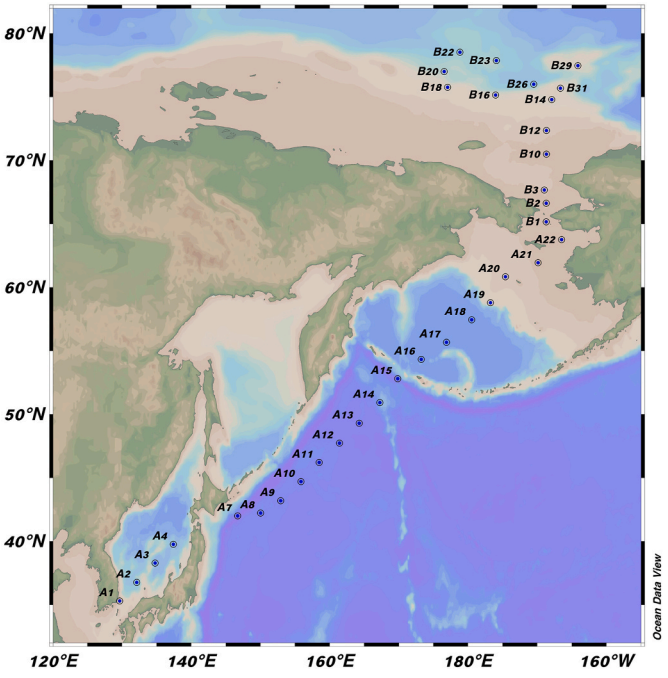

Fig. 1. Sampling stations during cruise ARA07 conducted in 2016. Stations labeled with "A" were sampled during Leg-A and those labeled with "B" were sampled during Leg-B.

labeled with "B" were sampled during Leg-B. For Leg-A and Leg-B, surface seawater was collected. Seawater from the subsurface chlorophyll maximum (SCM) depth was only collected for Leg-B. Procedures for sample collection were described in Xu et al. (2020). To summarize, seawater was collected at each station using Niskin bottles attached to a CTD rosette that measured the seawater temperature and salinity *in situ*. Approximately 5L of seawater was prefiltered through a 200 μm mesh (Nitex) to remove large plankton, and then sequentially filtered through 47-mm diameter 20 μm, 3 μm, and 0.4 μm pore size membrane (Millipore) filters to collect microeukaryotes of 0.4–3 μm, 3–20 μm, and 20–200 μm, respectively. The filters were flash-frozen in liquid nitrogen and kept at −80 °C until nucleic acid extraction.

Measurements on size-fractionated chlorophyll *a* (Chl *a*) concentrations, nutrients, and numeration on picoplankton, including heterotrophic bacteria (HBs), *Prochlorococcus*, and pigmented picoeukaryotes (PPEs), were introduced in Xu et al. (2020). Data on nutrients and picoplankton data were available only for Leg-B samples.

2.2. RNA extraction, PCR amplification, and sequencing

RNA was extracted using the RNeasy Mini Kit (Qiagen, USA) following the manufacturer's instructions and reverse transcribed into cDNA using the QuantiTect® Reverse Transcription Kit (Qiagen, USA). To amplify the hypervariable V4 regions of the SSU rRNA gene, the universal eukaryotic primers TAReuk454FWD1 and TAReukREV3 were employed (Stoeck et al., 2010). Each sample was PCR amplified four times to acquire sufficient amplicons for sequencing, and the PCR conditions followed Xu et al. (2020). The PCR amplicons for each sample were pooled and then purified using the MiniElute Gel Extraction Kit (Promega, China). Sequencing was performed at Majorbio (Shanghai, China) for paired-end sequencing (2 × 250) using an Illumina MiSeq platform. Leg-B surface water data were obtained from our previous work (Xu et al., 2020, accession number PRJNA596339), and the remaining data were uploaded to the NCBI Sequence Read Archive (accession number PRJNA800585).

2.3. Sequence processing

Quality filtering, demultiplexing, and assembly of raw data were done using Trimmomatic (Bolger et al., 2014) and Flash (Magoc and Salzberg, 2011), according to the criteria specified in Li et al. (2018). Dereplication of quality-filtered reads was then performed using Usearch 11 (Edgar, 2010). After screening reads with Mothur, only those between 300 and 500 bp were retained for downstream analysis (Schloss et al., 2009). Reads were denoised and clustered into zero-radius OTUs (ZOTUs) using UNOISE3 (Edgar, 2016a). ZOTUs with fewer than four reads were discarded. SINTAX (Edgar, 2016b) was used to classify ZOTUs against the PR2 database (Guillou et al., 2012). The generation of ZOTU tables was done in Usearch 11, and non-Eukaryota affiliated ZOTUs were deleted.

Because a functional analysis based on comprehensive annotations of nutritional modes of different groups of microeukaryotes is beyond the scope of this work, the ZOTUs identified were classified into four trophic functional groups, *i.e.*, phototrophs, heterotrophs, mixotrophs, and parasites, according to Armeli Minicante et al. (2019) and Schneider et al. (2020) (Supplementary Table S3).

2.4. Statistical analyses

To normalize sampling effort, ZOTU counts were rarefied at the lowest read number (39,870) across all samples before downstream analysis. Alpha diversity estimates, including ZOTU richness, Shannon, and phylogenetic diversity (PD), were calculated in QIIME (Caporaso et al., 2010). The Spearman correlation coefficients between the alpha diversity estimates and environmental factors were calculated using SPSS v.11.5 (SPSS, Chicago, IL, United States). The ordination of the microeukaryote community was visualized using principal coordinate analysis (PCoA) based on Bray-Curtis dissimilarities and unweighted UniFrac distances in R using the "vegan" package (R Core Team, 2015). Differences between sample groups were tested using analysis of similarity (ANOSIM) within PRIMER 6 (Clarke and Gorley, 2009). The Mantel and partial Mantel tests were used to explore correlations between environmental parameters and beta diversity in R with the "vegan" package (Legendre and Legendre, 1998).

Quantification of major ecological processes followed Stegen et al. (2013). Briefly, two major steps were conducted. We first calculated the β-nearest taxon index (βNTI) for all pairwise community comparisons to determine the influence of selection. Then, using Bray-Curtis-based Raup-Crick (RCbray) for pairwise community comparisons, the influences of dispersal and drift were calculated.

2.5. Network analysis

To reduce the complexity of the datasets, networks were constructed using ZOTUs with a relative abundance higher than 0.01% and detected in at least 10% of samples. The Spearman correlations among chosen ZOTUs were calculated using the 'Hmisc' (Harrell, 2008) and 'igraph' packages (Csardi and Nepusz, 2006). Correlations between ZOTUs that were significant (P-value < 0.01) and robust ($\rho \geq 0.6$) were exported as a GML format network file (Ju et al., 2014; Salazar et al., 2015). Prior to that, to reduce false-positive results, the P-values for each network were adjusted with a multiple testing correction using the Benjamini-Hochberg false discovery rate (FDR) control process (Benjamini et al., 2006). Network visualization, modular analysis, and network-level topological properties (*i.e.*, node, edge, average degree, density, diameter, clustering coefficient, and average path length) were conducted using Gephi v 0.9.2 (Bastian et al., 2009).

3. Results

3.1. Environmental parameters

Pronounced gradients in physical, chemical, and biological parameters were found along the transect from the northwest Pacific Ocean to the Arctic Ocean. Surface seawater temperature and salinity decreased with increasing latitude (Figure S2A). Water temperatures dropped from 25.3 °C in the East Sea of Korea to 4.5 °C in the Bering Strait, while they were below 0 °C in the Arctic Ocean. Salinity in Leg-A surface waters ranged from 30.6 to 33.6 and was below 30.0 in the Arctic Ocean. Water temperature ranged between −1.6 and 3.0 °C and salinity ranged between 30.7 and 32.4 at the SCM depth of the Leg-B. The Chl *a* concentration in surface waters followed a unimodal pattern along the transect (on average 0.35 μg/L and ranged from 0.04 to 1.21 μg/L), peaking at station A18 (Figure S2B). In the SCM depth, the Chl *a* concentration ranged between 0.42 and 2.14 μg/L. In the majority of Leg-A stations, picoplankton contributed the most to total Chl *a*, whereas microplankton dominated the SCM phytoplankton communities (Figure S2B).

Ammonium (NH_4), nitrate (NO_3), and nitrite (NO_2) concentrations in Leg-B surface waters were low, with practically all of them below the detection limit. Concentrations of NH_4, NO_3/NO_2, phosphate (PO_4), and silicate (SiO_2) were found to be higher in the SCM depth. The abundance of HBs varied between 1.53×10^5 and 1.27×10^6 cells/mL in surface water and between 1.27×10^5 and 1.01×10^6 cells/mL in SCM. PPEs were usually more abundant in the SCM than in the surface water (2.12×10^3–8.70×10^3 vs. 1.10×10^3–1.46×10^4 cells/mL) (Figure S3).

3.2. Alpha diversity estimates and the driving factors

To reveal the variations in active microeukaryote communities along a latitudinal gradient, 120 samples were analyzed using HTS of PCR-amplified SSU rRNA. A total of 10,542,320 quality-screened, Eukaryota-affiliated sequences were generated, ranging from 39,870 to

120,422 per sample (Table S2). The rarefaction curves based on ZOTU richness showed that microeukaryotes were not thoroughly sampled in most samples. However the pooled size-fractionated samples showed a symbol of saturation (Figure S1). A total of 11,908 ZOTUs were recovered, with the number of ZOTUs per sample ranging from 243 (A13p) to 3,207 (A9m). Following random subsampling at the lowest sequence count (39,870), a total of 10,556 ZOTUs were retrieved, ranging from 165 (A13p) to 2,607 (A9m) ZOTUs per sample (Fig. 2, Table S2).

Alpha diversity estimates for micro-sized (MS) microeukaryotes in surface water indicated that they peaked around mid-latitude (50–60 N). Alpha diversity estimates of the nano-sized (NS) fraction declined as latitude increased toward the north pole, with the minimum at the Arctic Circle. In comparison, those belonging to the pico-sized (PS) fraction increased slightly from low latitude, peaked between 50 and 60 N, and subsequently decreased toward the north pole (Fig. 2). For Leg-A, the alpha diversity estimates for PS and NS were comparable statistically, both being significantly higher than those for MS (Figure S4A). For Leg-B surface water samples, NS had significantly higher alpha diversity estimates than MS, but the differences between PS and NS, PS and MS were not significant (Figure S4B). The alpha diversity estimates for Leg-B SCM samples were comparable among MS, NS, and PS (Figure S4C).

Except for the MS, Spearman correlation analysis showed that the alpha diversity estimates of both PS and NS communities were significantly correlated with longitude, temperature, and salinity (Table 1).

3.3. Beta diversity, taxonomic and functional community compositions

In the two-dimensional principal coordinates analysis (PCoA) plots based on Bray Curtis distance and Unweighted Unifrac metric, all samples were clustered into two groups, *i.e.*, Group Leg-A, which included all surface water samples from Leg-A, and Group Leg-B, which included all samples from Leg-B (Fig. 3A), which was statistically supported (ANOSIM, $R = 0.60$, $p < 0.001$). Within Group Leg-A, samples were clustered according to the size of the microeukaryote assemblages (ANOSIM, $R = 0.63$, $p < 0.001$) (Fig. 3; S5A,B,C). Within Group Leg-B, samples were initially clustered by depth (ANOSIM, $R = 0.43$, $p < 0.001$), *i.e.*, surface water and SCM, and then by size (Fig. 3B; S4D, ANOSIM, $R = 0.53$, $p < 0.001$ for surface water and $R = 0.38$, $p < 0.001$ for SCM samples, respectively). The clustering dendrogram based on Bray Curtis dissimilarities revealed that all three size-fractionated microeukaryote subcommunities exhibited a regional clustering pattern apportioned to the oceanic regions (Fig. 4).

For the MS (Fig. 5; Figure S6A), Alveolata (mostly Class Spirotrichea, Ciliophora) accounted for ca. 37.7%, 37.0%, 18.3% in the Leg-A, Leg-B surface, and Leg-B SCM groups, respectively. Stramenopiles-affiliated sequences, largely associated with Bacillariophyta, contributed ca. 16.7% to Leg-A, compared to ca. 38.0% to Leg-B surface and ca. 53.8% to Leg-B SCM. Opisthokonta-affiliated sequences, mostly Arthropoda, contributed ca. 42.5% to Leg-A, followed by ca. 22.3% to Leg-B surface and ca. 12.7% to Leg-B SCM. Other groups contributed only minorly to the MS, with a few exceptions in individual samples. For example, Rhizaria accounted for ca. 14.5% of Leg-B SCM, particularly in sample BD29 (Figure S6A). For the NS (Fig. 5; Figure S6B), Alveolata (mostly Dinophyceae in Leg-A and Leg-B SCM, Spirotrichea in Leg-B surface) accounted for ca. 31.7%, 25.1%, and 42.6% in Leg-A, Leg-B surface, and Leg-B SCM, respectively. Stramenopiles (mostly Bacillariophyta) accounted for ca. 31.6%, 52.7%, and 41.2%, respectively, in the three groups. Opisthokonta accounted for ca. 11.1%, 8.8%, and 3.6%, respectively. Rhizaria was distributed uniformly, while Hacrobia was distributed unevenly, with a substantially higher proportion in Leg-A than in both Leg-B surface and Leg-B SCM. For the PS (Fig. 5; Figure S6C), Alveolata accounted for ca. 35.2%, 48.4%, and 42.9%, respectively, in Leg-A, Leg-B surface, and Leg-B SCM, with Spirotrichea continuing to be the major contributor. Stramenopiles accounted for ca. 20.6%, 34.5%, and 31.3% of the total, respectively. Opisthokonta and Hacrobia were more prevalent in Leg-A surface samples than in Leg-B surface and Leg-B SCM samples.

In terms of ZOTU richness, Alveolata (ca. 42.4%, mainly Ciliophora and Dinophyceae) and Stramenopiles (ca. 27.0%, mainly Bacillariophyta) were the dominant groups in the MS, followed by Opisthokonta (ca. 12.4%, mainly Arthropoda), Rhizaria (ca. 7.9%, mainly Acantharea), and other groups in Leg-A (Fig. 5, Fig. S7A). In Leg-B surface samples, Stramenopiles (ca. 40.1%, mainly Bacillariophyta) surpassed Alveolata (ca. 36.2%, mainly Ciliophora) as the most prominent group, followed by Rhizaria (ca. 10.6%, mainly Cercozoa), and other groups. Alveolata (ca. 38.8%, mainly Ciliophora) was the most prevalent group in Leg-B SCM, followed by Stramenopiles (35.2%, mainly Bacillariophyta), Rhizaria (ca. 16.4%, mainly Cercozoa), and other groups. For the NS (Fig. 5, Figure S7B), the three most dominant groups in Leg-A were Alveolata (ca. 40.5%, mainly Syndiniales), Stramenopiles (ca. 23.3%, mainly Bacillariophyta), and Rhizaria (ca. 13.0%, mainly Polycystinea), while those in Leg-B surface were Stramenopiles (ca. 34.5%, mainly Bacillariophyta), Alveolata (ca. 32.3%, mainly Dinophyceae and Ciliophora), and Rhizaria (ca. 14.5%). For Leg-B SCM, Alveolata (mainly Dinophyceae) and Stramenopiles (mainly Bacillariophyta) accounted for ca. 43.2% and 31.4%, respectively, followed by Rhizaria (ca. 12.9%,

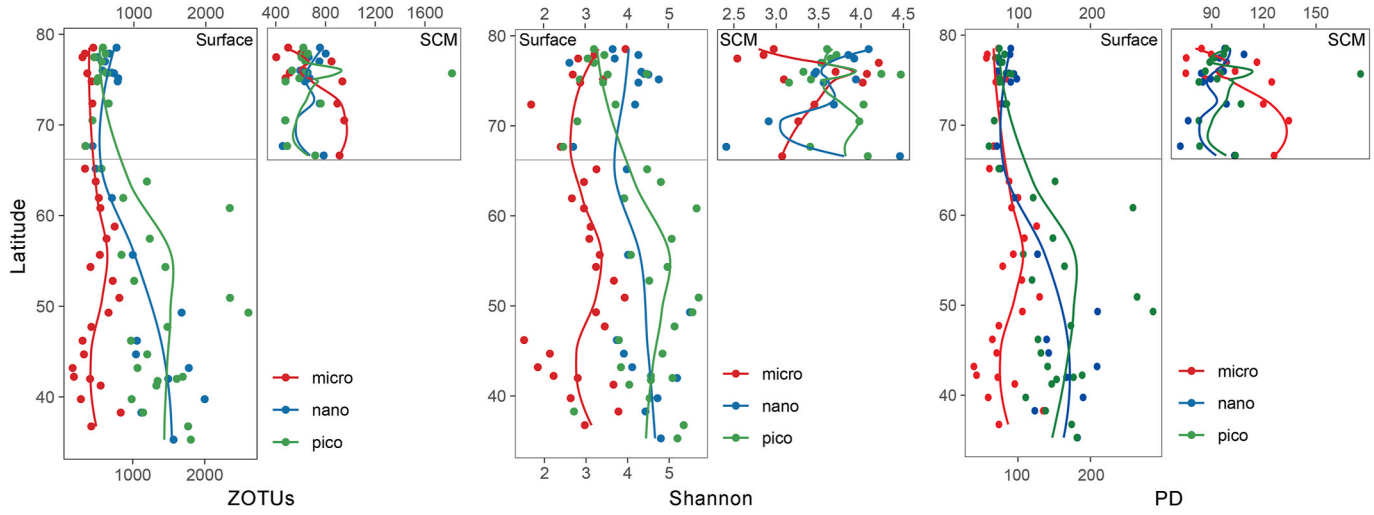

Fig. 2. Latitudinal trends of alpha diversity estimates (ZOTU richness, Shannon, and PD) of size fractionated microeukaryotes in the surface water and the SCM depth.

Table 1
Spearman's correlation coefficients between alpha diversity estimates and environmental variables. Significant values of p (<0.05) are in bold.

Variable		Micro			Nano			Pico		
		OTUs	Shannon	PD	OTUs	Shannon	PD	OTUs	Shannon	PD
Latitude	r	0.174	0.175	−0.042	−0.497	−0.360	−0.515	−0.667	−0.590	−0.680
	p	0.282	0.281	0.796	**0.003**	**0.037**	**0.002**	**0.000**	**0.000**	**0.000**
Longitude	r	−0.113	0.199	−0.141	0.374	0.008	0.280	0.301	0.255	0.268
	p	0.488	0.219	0.386	0.029	0.963	0.109	**0.042**	0.088	0.072
Temperature	r	−0.181	−0.235	0.023	0.507	0.371	0.558	0.662	0.574	0.681
	p	0.264	0.144	0.889	**0.002**	**0.031**	**0.001**	**0.000**	**0.000**	**0.000**
Salinity	r	0.110	0.108	0.244	0.568	0.094	0.534	0.608	0.517	0.611
	p	0.500	0.506	0.130	**0.000**	0.596	**0.001**	**0.000**	**0.000**	**0.000**
Chl *a*	r	0.400	0.270	0.275	0.0416	−0.402	0.049	0.509	0.462	0.548
	p	**0.011**	0.091	0.086	0.815	**0.018**	0.783	**0.000**	**0.001**	**0.000**

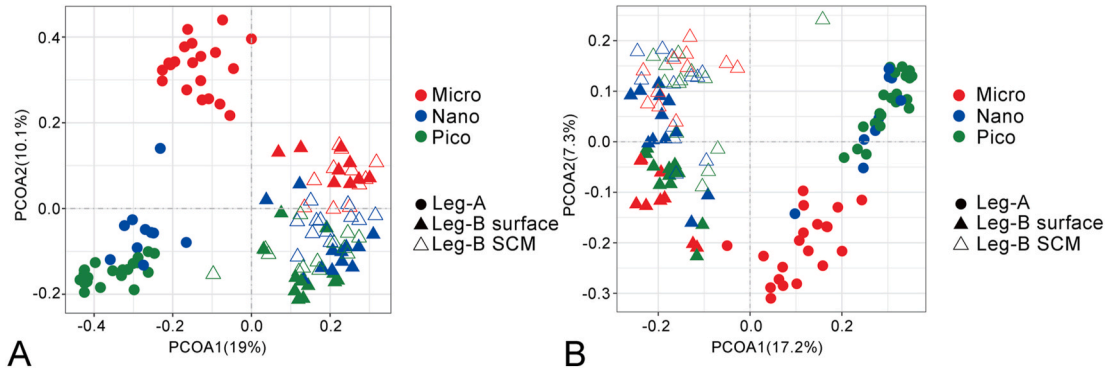

Fig. 3. Plots of principal coordinates analysis (PCoA) of microeukaryote communities based on Bray Curtis dissimilarities (A) and Unweighted UniFrac distance matrices (B).

mainly Cercozoa) and other groups. For the PS (Fig. 5, Figure S7C), Alveolata (ca. 37.0%, mainly Spirotrichea and Syndiniales), Stramenopiles (ca. 22.9%, mainly Bacillariophyta), and Hacrobia (ca. 15.3%, mainly Prymnesiophyceae) were the top three contributors in Leg-A. For Leg-B surface, Alveolata (ca. 42.0%, mainly Ciliophora) was the most abundant group, followed by Stramenopiles (ca. 28.7%, mainly Bacillariophyta), Rhizaria (ca. 11.2%, mainly Cercozoa), and other groups. While for Leg-B SCM, Alveolata (mainly Syndiniales) and Stramenopiles (mainly Bacillariophyta) were the two most dominant groups, followed by Rhizaria (ca. 12.4%, mainly Cercozoa) and other groups.

The simple Mantel test revealed that microeukaryote communities in all three fractions were significantly correlated with water temperature, latitude, and salinity (Table 2). After controlling for latitude, all three fractions were still significantly correlated with temperature but with lower R values. After controlling for temperature, only the MS showed a weak correlation with latitude, and no significant correlations were found between NS/PS and latitude (Table 2).

3.4. Variations in the richness of the functional groups

For the MS, the proportion of heterotrophs affiliated reads decreased along the transect while phototrophs increased. The proportion of mixotrophs was the highest in the Leg-B surface, followed by Leg-A and Leg-B SCM (Fig. 6; S8). For the NS, the mixotrophs were the highest contributors in Leg-A, whereas phototrophs took over in Leg-B surface and Leg-B SCM. In all three groups, mixotrophs dominated the PS (Fig. 6, S8). In terms of richness, Leg-B SCM had the highest ZOTU number of heterotrophs, phototrophs, and mixotrophs for the MS. Leg-A had the highest ZOTU number of any of the four functional groups in the NS and PS (Fig. 6, S9).

3.5. Co-occurrence networks

Co-occurrence networks for Leg-A, Leg-B surface, and Leg-B SCM were constructed, respectively (Fig. 7). The Leg-A network had 657 nodes and 18,963 edges, with 96.97% of network connections being positive. The Leg-B surface network had 443 nodes and 6054 edges, with 91.13% of network connections being positive, whereas the Leg-B SCM network contained 511 nodes and 5688 edges, with 86.74% of network connections being positive (Table S4). The Leg-A network had the highest network density, followed by the Leg-B surface network and the Leg-B SCM network. In comparison, the Leg-B SCM network had the highest modularity and average path length, followed by the Leg-B surface network and the Leg-A network (Table S4). Unique node-level topological features of the three networks were compared. Leg-A had the highest degree, closeness centrality, and harmonic closeness centrality, followed by the Leg-B surface network and the Leg-B SCM network (Figure S10). Significantly higher betweenness centrality values were found for the Leg-A network than the other two networks. No significant betweenness centrality values were found between the Leg-B surface network and the Leg-B SCM network (Figure S10).

Spirotrichea (Ciliophora, 14.3%), non-diatom Stramenopiles (10.4%), Prymnesiophyceae (9.9%), Dinophyceae (9.4%), and Bacillariophyta (8.7%) were the highest contributors to the Leg-A network, accounting for more than half of all nodes (Fig. 7A). Bacillariophyta (19.4%), Spirotrichea (15.8%), Cercozoa (12.9%), and non-diatom Stramenopiles (8.8%) dominated the Leg-B surface network, contributing ca. 57% of all nodes. Bacillariophyta (21.9%), Spirotrichea (15.3%), Dinophyceae (11.2%), and Cercozoa (10.0%) contributed the most to the Leg-B SCM network, accounting for ca. 58.4% of all nodes (Fig. 7A). Mixotrophs dominated both the Leg-A and Leg-B SCM networks (ca. 45.5% and 38.0% of total nodes, respectively). Heterotrophs contributed almost equally to the Leg-A and Leg-B SCM networks (ca. 28.5% and 29.2%, respectively). Heterotrophs and mixotrophs

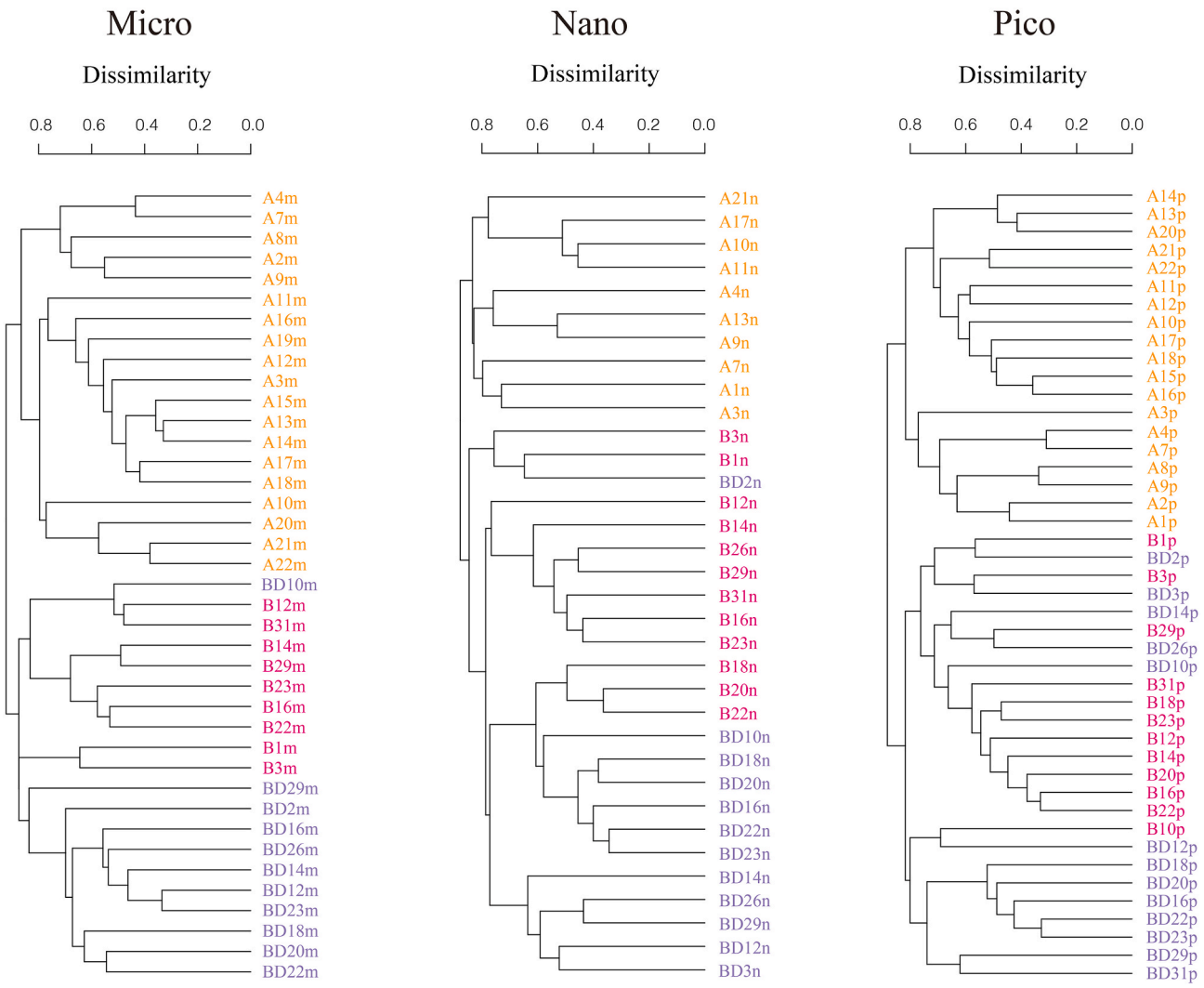

Fig. 4. Bray Curtis dissimilarity clustering of size fractionated microeukaryotes of Leg-A (orange), Leg-B surface (purple), and Leg-B SCM (blue) waters, respectively. (For interpretation of the references to color in this figure legend, the reader is referred to the Web version of this article.)

contributed about equally to the Leg-B surface network (ca. 35.2% and 32.3%, respectively), followed by phototrophs (27.4%) and parasites (ca. 2.9%) (Fig. 7B). The Leg-A network was parsed into five modules, while the five most abundant modules in the Leg-B surface and SCM networks accounted for ca. 94.1% and 85.1% of all nodes, respectively (Fig. 7C).

3.6. Community assembly processes

Dispersal limitation was identified as the primary driver for community assembly processes in the active microeukaryote communities, explaining ca. 57.9%, 63.3%, and 53.7% of community turnover in the micro-, nano-, and pico-sized fractions, respectively (Fig. 8). Drift surpassed other processes as the second most important driving process in micro- and nano-sized communities (ca. 32.2% and 15.5%, respectively), while in pico-sized communities, heterogeneous selection accounted for ca. 18.6% of community turnover, followed by drift (ca. 14.9%) and other processes (Fig. 8).

4. Discussion

4.1. Latitudinal diversity gradient (LDG) of the active microeukaryotes

The LDG refers to the increase in species richness toward the tropics for terrestrial, freshwater, and marine organisms, a phenomenon that has captivated ecologists for decades and is still a source of contention (Willig et al., 2003; Hillebrand, 2004; Endo et al., 2018; Ibarbalz et al., 2019; Moss et al., 2020). Even when samples are obtained concurrently, different groups of microorganisms may exhibit diverse LDG patterns (Endo et al., 2018; Ibarbalz et al., 2019). To our best knowledge, this is the first time an attempt has been made to address the LDG of active microeukaryotes using environmental RNA sequencing. Focusing on surface waters, we found that alpha diversity estimates for nano- and pico-sized eukaryotes decreased with increasing latitude, consistent with prior DNA-based sequencing studies (Ibarbalz et al., 2019). Our study found no evidence of decreasing trends in the micro-sized fraction toward the Arctic pole, consistent with a previous study using samples taken along a Pacific transect (Moss et al., 2020). It is worth noting that the samples included in this study did not include any from the tropical region. Thus, estimations of the alpha diversity of microeukaryotes in the tropical ocean require more investigation. It has been suggested that patterns of diversity along the latitudinal gradient may be dependent on spatial scale and taxonomic hierarchy (*i.e.*, different groups of marine microorganisms may respond differently to the latitudinal changes) and may even be seasonal dependent (Ladau et al., 2013). The results may be biased by the heterogeneous datasets, such as meta-analyses based on samples taken from different ocean regions, different seasons/expeditions, or targeted groups of marine microorganisms, or even

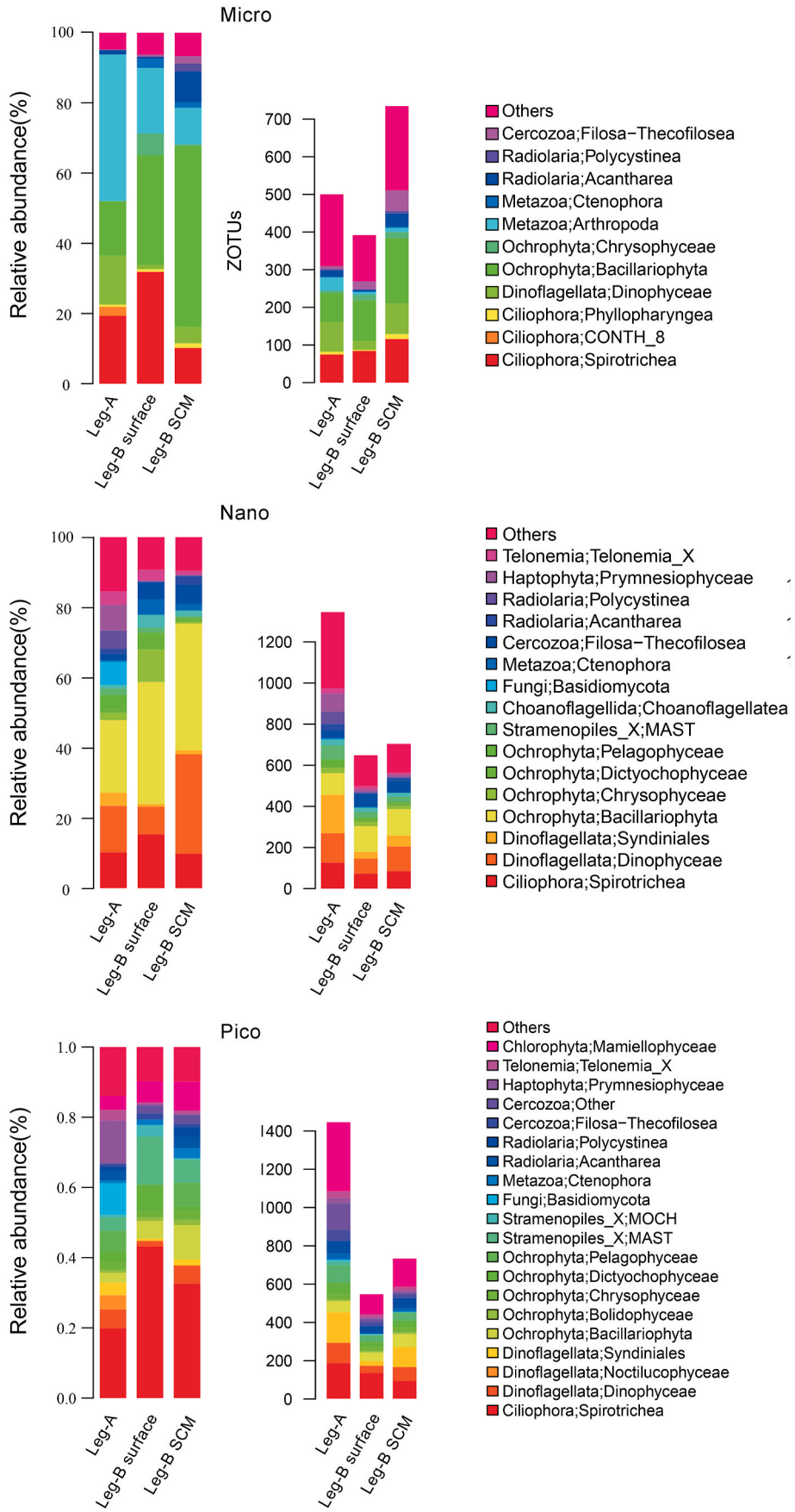

Fig. 5. Variations in sequence proportions (upper) and ZOTU richness (lower) of size fractionated microeukaryotes.

Table 2
Simple and partial Mantel tests for the correlations between environmental factors and microeukaryote communities.

	Mantel Test					
Environmental factors	Micro		Nano		Pico	
	R	*p*	*R*	*p*	*R*	*p*
Latitude	0.568	**0.001**	0.468	**0.001**	0.366	**0.001**
Longitude	0.068	0.054	0.035	0.268	0.066	0.053
Temperature	0.611	**0.001**	0.526	**0.001**	0.416	**0.001**
Salinity	0.160	**0.007**	0.285	**0.002**	0.056	0.176
Chl *a*, total	0.044	0.216	−0.061	0.736	0.094	0.073
Chl *a* (>20 μm)	0.142	**0.019**	−0.188	0.974	0.090	0.102
Chl *a* (2–20 μm)	0.007	0.548	0.093	0.105	0.142	**0.009**
Chl *a* (<2 μm)	0.025	0.297	0.210	**0.007**	0.268	**0.002**
	Partial Mantel Test (control for latitude)					
Environmental factors	Micro		Nano		Pico	
	R	*p*	*R*	*p*	*R*	*p*
Longitude	−0.122	1	−0.049	0.811	−0.024	0.711
Temperature	0.283	**0.001**	0.277	**0.001**	0.213	**0.001**
Salinity	0.011	0.405	0.210	**0.010**	−0.047	0.753
Chl *a*, total	0.062	0.128	−0.016	0.554	0.127	**0.029**
Chl *a* (>20 μm)	0.207	**0.002**	−0.141	0.934	0.138	**0.039**
Chl *a* (2–20 μm)	−0.029	0.678	0.111	0.081	0.149	**0.006**
Chl *a* (<2 μm)	−0.002	0.522	0.205	**0.007**	0.266	**0.001**
	Partial Mantel Test (control for temperature)					
Environmental factors	Micro		Nano		Pico	
	R	*p*	*R*	*p*	*R*	*p*
Latitude	0.071	0.061	−0.052	0.859	−0.023	0.706
Longitude	0.021	0.682	−0.024	0.639	0.017	0.319
Salinity	−0.030	0.687	0.203	**0.014**	−0.069	0.879
Chl *a*, total	0.015	0.375	−0.014	0.556	0.117	**0.029**
Chl *a* (>20 μm)	0.173	**0.004**	−0.132	0.899	0.128	0.058
Chl *a* (2–20 μm)	−0.048	0.831	0.108	0.090	0.150	**0.007**
Chl *a* (<2 μm)	−0.042	0.824	0.171	**0.021**	0.258	**0.001**

different sources of nucleic acid (DNA vs. RNA). Thus, future international collaborations based on large-scale, seasonal sampling, and multiple approaches will shed further insight on the LDG of various microbial groups.

4.2. Latitudinal variation in the composition of the active microeukaryote assemblages

Early research has emphasized the importance of water masses in determining the distribution of microeukaryotes (Yang et al., 2020; Sun et al., 2020, 2021; Gu et al., 2021). The sampling area in this study covers the East Sea of Korea, the northwest Pacific Ocean, the Bering Sea, and the Arctic Ocean. Stations A1-A4 were primarily influenced by a branch of the Kuroshio Current, which brings warm, nutrient-depleted water from the north equatorial region, as indicated by the relatively low Chl *a* concentration. Stations A7-A18 are mainly affected by the mixing of the cold Oyashio Current and the Kuroshio Current (Hunt et al., 2016). The Oyashio Current is rich in nutrients and biologically productive, as shown by the relatively high Chl *a* concentration (Figure S1) and the high relative sequence abundance of diatoms observed (Figure S6B). A19-B10 were mostly influenced by warm waters from the northern Pacific Ocean, including the Alaskan Coastal Current (Hunt et al., 2016). The complex water masses and mixing of multiple water masses within the sampling area may help explain the sharp shifts of the microeukaryote communities observed, particularly those in Leg-A (Fig. 3, S6).

Latitudinal variation in the composition of the active microeukaryote assemblage was observed. Both PCoA plots using Bray Curtis dissimilarities and the Unweighted Unifrac metric showed that Leg-A, Leg-B surface, and Leg-B SCM harbored distinct communities (Fig. 3). Previous studies have shown clear distinctions in microeukaryote communities found within and outside of the Arctic Ocean, as well as between surface and SCM waters in the Arctic Ocean (Bachy et al., 2011; Lovejoy and Potvin, 2011; Monier et al., 2013; Sun et al., 2022). Metazoa, primarily represented by Arthropoda, were major contributors to the micro-sized fraction, and their contribution to total sequences decreased toward the Arctic pole (Fig. 5). The predominance of Arthropoda-affiliated sequences in the micro-rather than nano/pico-sized fractions was expected, as arthropods were key components of microzooplankton (Matsuno et al., 2012). Additionally, our study showed that using RNA-based sequencing to conduct protistan surveys might help reduce the interference caused by metazoan sequences (Xu et al., 2017). Focusing on surface water, the proportion of Bacillariophyta (Diatom)-affiliated sequences generally increased toward the Arctic, for both the micro- and nano-sized eukaryotes. Diatoms have been identified as the main phytoplankton group during Arctic spring blooms and have been shown to serve a critical role as primary producers in high latitude marine ecosystems, both in sea ice and seawater (Lovejoy et al., 2002; Vaquer-Sunyer et al., 2013). Most diatom species described to date have been found in the micro- and nano-sized fractions (Katsuki et al., 2009; Zheng et al., 2011). Ciliophora, mainly represented by Spirotrichea, was the dominant group and contributed increasingly to each of the three size fractions as latitude increased (Fig. 5). Spirotrichea is primarily comprised of aloricate oligotrichs, which are the primary herbivores in planktonic food webs (Montagnes and Lynn, 1991). In the open ocean, they often consisted of small (sometimes <20 μm) *Strombidium*, *Strobilidium*, *Leegardiella*, and other species. (Montagnes and Lynn, 1991;

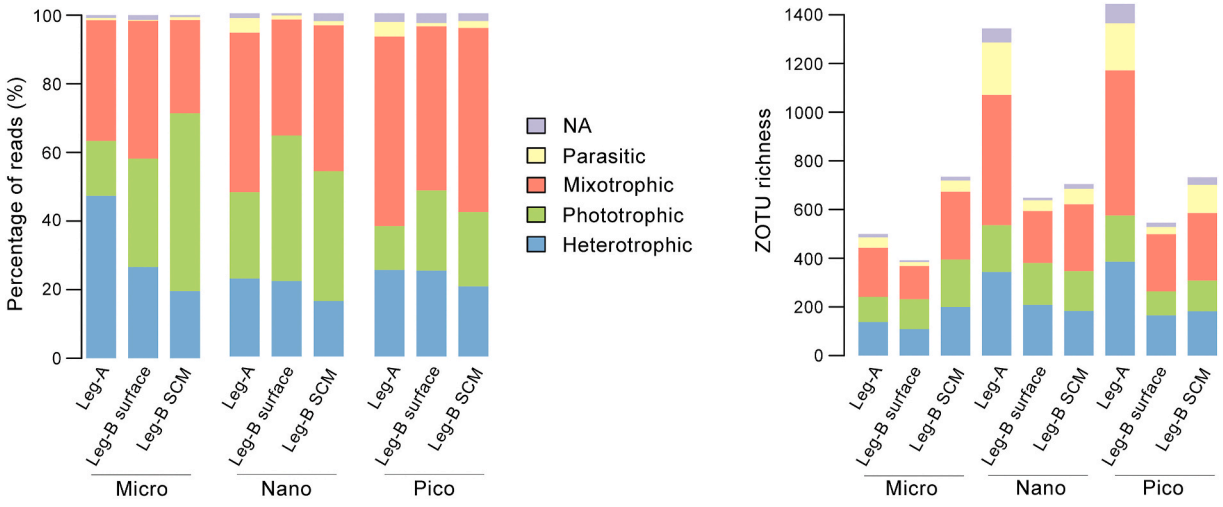

Fig. 6. Variations in sequence proportions and ZOTU richness of different functional groups.

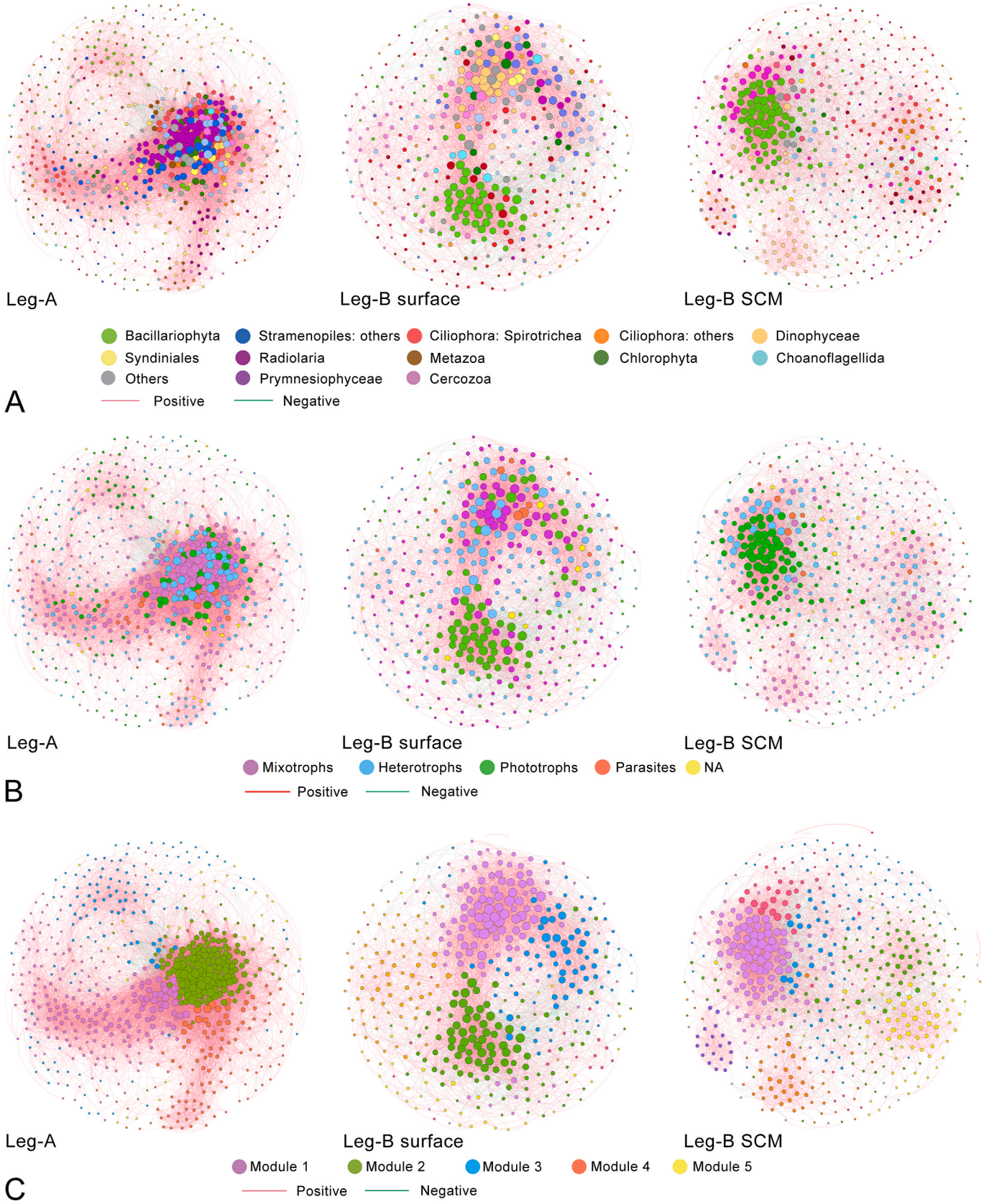

Fig. 7. The co-occurrence patterns among ZOTUs in Leg-A, Leg-B surface, and Leg-B SCM by network analysis. The nodes were colored according to taxonomic (A), functional (B) identities, and modularity classes (C).

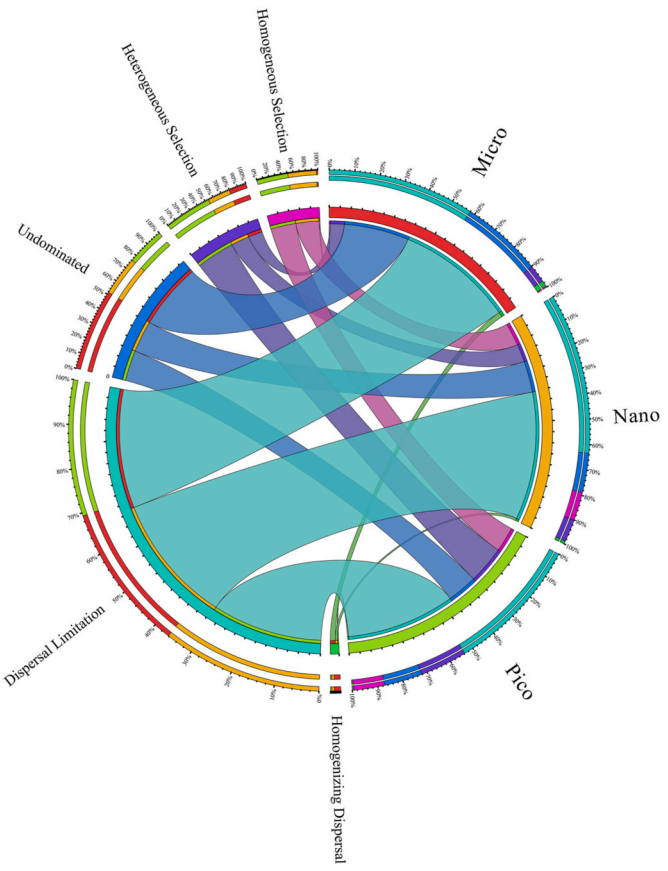

Fig. 8. Partition of community assembly process of the size-fractionated microeukaryotes.

Sherr et al., 2013; Sun et al., 2019; Huang et al., 2021). Small spirotrichs were previously shown to be important components of the Arctic microzooplankton community and to be active grazers of phytoplankton, including diatoms (Sherr et al., 2003, 2013; Stoecker et al., 2014; Jiang et al., 2015; Xu et al., 2018b). Except for heterotrophic ciliates, mixotrophic spirotrichs (*e.g.*, *Laboea strobila*) have been reported to dominate ciliate assemblages in the Arctic, contributing significantly to primary production (Stoecker and Lavrentyev, 2018). The contributions of ciliate-affiliated sequences in the SCM were lower than those in the Leg-B surface but comparable to those in Leg-A, consistent with a previous report that mixotrophic ciliates were also significant contributors to Chl *a* in the SCM (Franzè and Lavrentyev, 2017). The higher proportions of ciliate-affiliated sequences at the surface than at the SCM depth in Leg-B were also consistent with a previous report based on an RNA survey showing a rise in the relative abundance of ciliate-affiliated sequences in the surface waters beginning in early June (Onda et al., 2017). The increasing contribution of spirotrichs to our dataset along the transect indicated that they were also transcriptionally active, which corroborated prior findings indicating ciliates were major players in the microbial food web of the Arctic Ocean (Sherr et al., 2003).

Previous studies employing microscopy observations revealed that dinoflagellates predominate in the Arctic during summer (Booth and Horner, 1997; Gradinger, 1999; Olli et al., 2007). This study found that Dinophyceae-affiliated sequences were more numerous in the SCM than in the surface waters in all three size fractions (Fig. 5), which is consistent with a previous report showing that the proportions of dinoflagellate-affiliated sequences increased in the SCM, compared to the surface waters (Onda et al., 2017). Using DNA-based clone library sequencing, one study showed that the contribution of Dinokaryota to deep waters increases during polar nights (Bachy et al., 2011). Bacillariophyta predominated over dinoflagellates in both the surface water and SCM of the Arctic, consistent with a previous study (Crawford et al., 2018).

Haptophyta, mainly Prymnesiophyceae, were the dominant group in both the nano- and pico-sized fractions of the Leg-A samples, with their contribution to the total sequence counts averaging ca. 12% in the pico-sized fraction (Fig. 5). Prymnesiophyceae are abundant in marine environments and often dominate the eukaryotic phytoplankton pigment pool in temperate/tropical/subtropical waters (Liu et al., 2009; Xu et al., 2018a). Many Prymnesiophyceae species are found in pico- and nano-sized fractions, and their ability to participate in both phototrophy and phagotrophy is thought to give them and advantage over other obligate phagotrophs/phototrophs (Liu et al., 2009; Unrein et al., 2014). For example, in some *Chrysochromulina* species, feeding can enhance growth at low irradiance (Hansen and Hjorth, 2002). Our study found *Phaeocystis*, *Chrysochromulina*, *Prymnesium*, and the unidentified Prymnesiales in surface and SCM waters, which is consistent with a previous survey of Haptophyta along a Pacific transect (Endo et al., 2018). During the Arctic spring bloom, *Phaeocystis* accounted for more than 95% of all plankton cells (Vernet, 1991). Although members of *Phaeocystis* have not been shown to be phagotrophic, they have been proposed to contribute substantially to primary production, food source of metazoans, vertical carbon flux, and trace metal cycles in polar waters, including manganese, zinc, iron, and copper (Davidson and Marchant, 1987; Lubbers et al., 1990; Marchant and Thomsen, 1994).

Notably, MAST-affiliated sequences represented ca. 13.5% of all pico-sized eukaryotes in Leg-B surface waters, more than double the proportion seen in Leg-B SCM waters (ca. 6.5%) (Fig. 5). MASTs are widespread in the Arctic Ocean, where they act as active grazers of bacterial grazers and recycle carbon in the water column, as identified by sequencing and FISH approaches (Lovejoy et al., 2006; Comeau et al., 2011; Terrado et al., 2011; Monier et al., 2013; Thaler and Lovejoy, 2014). Using DNA environmental sequencing, previous studies have shown that MAST-affiliated sequences contribute more to the SCM than to Arctic surface waters, which is consistent with the current study (Monier et al., 2013).

4.3. Co-occurrence networks of the active microeukaryotes

The co-occurrence patterns of active microeukaryotes were explored in this work spanning a ca. 5000 km transect. The findings indicate that the co-occurrence networks of microeukaryotes in Leg-A, Leg-B surface, and Leg-B SCM groups have distinct compositions and structures (Fig. 7). The degree value was proposed to be a local quantification feature showing the number of direct co-occurrence interactions for a specific ZOTU (Greenblum et al., 2012). Significantly higher degree values were found in the Leg-A than in the Leg-B surface and Leg-B SCM networks, indicating that microeukaryotes outside the Arctic Ocean may have stronger correlations than those inside. Niche differentiation is one possibility for the observed network topological difference. The more geographically constrained sampling area in the Arctic Ocean may result in a more homogeneous ecosystem, causing weak niche differentiation. The weak niche differentiation may result in stronger interactions between microorganisms and increased competition, as shown by the presence of higher negative correlations in Leg-B surface and Leg-B SCM networks (Table S5). In comparison to the Arctic Ocean, the drastic environmental changes along the transect from the East Sea of Korea to the Bering Strait may result in higher niche differentiation. The high niche differentiation may avoid competition and allow the microorganisms to coexist within the same community (Ma et al., 2016; Mikhailov et al., 2019). Indeed, ca. 96.97% of correlations in the Leg-A network were positive, significantly higher than the correlations in the Leg-B surface and Leg-B SCM networks (ca. 91.13% and 86.74%, respectively) (Table S4).

The Leg-A network showed a large number of positive correlations among key microeukaryote groups, whereas the Leg-B surface and Leg-B

SCM networks did not (Table S5). For example, ca. 96.27% of correlations between Bacillariophyta and Spirotrichea were positive in the Leg-A network, whereas the Leg-B surface and Leg-B SCM networks had substantially lower correlations (ca. 55.99% and 66.10%, respectively). Bacillariophyta mainly consisted of phototrophic species, while species affiliated with Spirotrichea, such as *Strombidium* spp., *Loboea strobila*, and *Tontonia* spp., were capable of mixotrophy (Johnson and Beaudoin, 2019). The low positive correlations found between Bacillariophyta and Spirotrichea in the Arctic Ocean may imply that they may compete for resources, such as nutrients for growth. Indeed, mixotrophic spirotrichs have been repeatedly reported to be significant contributors to Arctic Ocean Chl *a* stocks as well as grazers of pico- and nano-sized phytoplankton (Putt, 1990; Sherr et al., 2013; Franzè and Lavrentyev, 2017). Cercozoa have previously been reported as a large protozoan group found in soil, freshwater, and marine environments (Bass and Cavalier-Smith, 2004). Members of this group may act as diatom and dinoflagellate parasites as well as grazers (Tillmann et al., 1999; Schnepf and Kuhn, 2000; Genitsaris et al., 2015). However, in this study, the correlations between cercozoan and diatom/dinoflagellate were mostly positive, indicating that cercozoans were probably not grazing/parasitizing on diatoms/dinoflagellates (Table S5). Interestingly, the negative correlations between Cercozoa and Spirotrichea increased in the Arctic Ocean, which may imply that they were competing for food with spirotrich ciliates, such as bacteria and nanoflagellates.

5. Conclusions

Based on a latitudinal transect sample collection from the Northwest Pacific Ocean to the central Arctic Ocean, we explored the diversity, community composition, and co-occurrence relationships of microeukaryote assemblages using environmental RNA extracts, followed by high throughput sequencing on the V4 regions of the reverse transcribed SSU rRNA gene. We found a latitudinal diversity gradient (LDG) for both nano- and pico-sized microeukaryotes, but not for the micro-sized fraction. The community composition and co-occurrence relationships of microeukaryotes were found to be distinct across stations outside and inside the Arctic Ocean, as well as between stations in the surface and subsurface chlorophyll maximum waters of the Arctic Ocean. Water temperature was identified as the most influential environmental factor shaping the alpha diversity estimates for nano- and pico-sized eukaryotes, as well as the top factor driving community composition in all three fractions. The microeukaryote community was primarily driven by dispersal limitation for all three size fractions.

Author statement

Xu Dapeng: Conceptualization, Supervision, Writing - Review & Editing, Resources, Funding acquisition; **Kong Hejun:** Writing - Original Draft, Formal analysis, Investigation; **Yang Eun-Jin:** Resources, Investigation, Funding acquisition; **Wang Ying:** Formal analysis; **Li Xinran:** Investigation; **Sun Ping:** Writing - Review & Editing, Formal analysis; **Jiao Nianzhi:** Resources, Funding acquisition; **Lee Youngju**: Investigation; **Jung Jinyoung**: Investigation; **Cho Kyoung-Ho**: Investigation

Funding

This work was supported by the National Natural Science Foundation of China (42188102, 41876142, 42141003, 41861144018, 31772426). This research was a part of the project titled 'Korea-Arctic Ocean Warming and Response of Ecosystem (K-AWARE, KOPRI, 1525011760)', funded by the Ministry of Oceans and Fisheries, Korea and the Asian Polar Science Fellowship Program 2020 awarded by the Korea Polar Research Institute to HK.

Declaration of competing interest

The authors declare that they have no known competing financial interests or personal relationships that could have appeared to influence the work reported in this paper.

Acknowledgment

We thank the captain, crew, and marine technicians of *R/V ARAON* for facilitating field sampling. We also thank the two anonymous reviewers for their valuable comments.

Appendix A. Supplementary data

Supplementary data to this article can be found online at https://doi.org/10.1016/j.envres.2022.113234.

References

Armeli Minicante, S., Piredda, R., Quero, G.M., Finotto, S., Bernardi Aubry, F., Bastianini, M., Pugnetti, A., Zingone, A., 2019. Habitat heterogeneity and connectivity: effects on the planktonic protist community structure at two adjacent coastal sites (the Lagoon and the Gulf of Venice, Northern Adriatic Sea, Italy) revealed by metabarcoding. Front. Microbiol. 10, 2736.
Azam, F., Malfatti, F., Azam, F., Malfatti, F., 2007. Microbial structuring of marine ecosystems. Nat. Rev. Microbiol. 5, 782–791.
Bachy, C., López-García, P., Vereshchaka, A., Moreira, D., 2011. Diversity and vertical distribution of microeukaryotes in the snow, sea ice and seawater near the North Pole at the end of the polar night. Front. Microbiol. 2, 106.
Bass, D., Cavalier-Smith, T., 2004. Phylum-specific environmental DNA analysis reveals remarkably high global biodiversity of Cercozoa (Protozoa). Int. J. Syst. Evol. Microbiol. 54, 2393–2404.
Bastian, M., Heymann, S., Jacomy, M., 2009. Gephi: an open source software for exploring and manipulating networks. In: International AAAI Conference on Weblogs and Social Media. AAAI Press, Menlo Park, CA, USA.
Beaugrand, G., Edwards, M., Raybaud, V., Goberville, E., Kirby, R.R., 2015. Future vulnerability of marine biodiversity compared with contemporary and past changes. Nat. Clim. Change 5, 695.
Benjamini, Y., Krieger, A.M., Yekutieli, D., 2006. Adaptive linear step-up procedures that control the false discovery rate. Biometrika 93, 491–507.
Bolger, A.M., Lohse, M., Usadel, B., 2014. Trimmomatic: a flexible trimmer for Illumina sequence data. Bioinformatics 30, 2114–2120.
Booth, B.C., Horner, R.A., 1997. Microalgae on the Arctic Ocean section, 1994: species abundance and biomass. Deep Sea Res. Part II Top. Stud. Oceanogr. 44, 1607–1622.
Bopp, L., Resplandy, L., Orr, J.C., Doney, S.C., Dunne, J.P., Gehlen, M., Halloran, P., Heinze, C., Ilyina, T., Seferian, R., Tjiputra, J., Vichi, M., 2013. Multiple stressors of ocean ecosystems in the 21st century: projections with CMIP5 models. Biogeosciences 10, 6225–6245.
Brun, P., Stamieszkin, K., Visser, A.W., Licandro, P., Payne, M.R., Kiørboe, T., 2019. Climate change has altered zooplankton-fuelled carbon export in the North Atlantic. Nat. Ecol. Evol. 3, 416–423.
Caporaso, J.G., Kuczynski, J., Stombaugh, J., Bittinger, K., Bushman, F.D., Costello, E.K., et al., 2010. QIIME allows analysis of high-throughput community sequencing data. Nat. Methods 7, 335–336.
Caron, D.A., Countway, P.D., Jones, A.C., Kim, D.Y., Schnetzer, A., 2012. Marine protistan diversity. Ann. Rev. Mar. Sci 4, 467–493.
Clarke, K.R., Gorley, R.N., 2009. PRIMER V6: User Manual/Tutorial. PRIMER–E, Plymouth.
Comeau, A.M., Lagunas, M.G., Scarcella, K., Varela, D.E., Lovejoy, C., 2019. Nitrate consumers in arctic marine eukaryotic communities: comparative diversities of 18S rRNA, 18S rRNA genes, and nitrate reductase genes. Appl. Environ. Microbiol. 85 e00247–19.
Comeau, A.M., Li, W.K.W., Tremblay, J.-E., Carmack, E.C., Lovejoy, C., 2011. Arctic Ocean Microbial community structure before and after the 2007 record sea ice minimum. PLoS One 6, e27492.
Crawford, D.W., Cefarelli, A.O., Wrohan, I.A., Wyatt, S.N., Varela, D.E., 2018. Spatial patterns in abundance, taxonomic composition and carbon biomass of nano- and microphytoplankton in Subarctic and Arctic Seas. Prog. Oceanogr. 162, 132–159.
Csardi, G., Nepusz, T., 2006. The igraph software package for complex network research. Inter Journal, Complex Systems 1695, 1–9.
Davidson, A.T., Marchant, H.J., 1987. Binding of manganese by Antarctic *Phaeocystis pouchetii* and the role of bacteria in its release. Mar. Biol. 95, 481–487.
de Vargas, C., Audic, S., Henry, N., Decelle, J., Mahé, F., Logares, R., et al., 2015. Eukaryotic plankton diversity in the sunlit ocean. Science 348, 1261605.
Dell'Anno, A., Danovaro, R., 2005. Extracellular DNA plays a key role in deep-sea ecosystem functioning. Science 309, 2179.
Edgar, R.C., 2010. Search and clustering orders of magnitude faster than BLAST. Bioinformatics 26, 2460–2461.
Edgar, R.C., 2016a. UNOISE2: Improved Error-Correction for Illumina 16S and ITS Amplicon Sequencing. bioRxiv.

Edgar, R.C., 2016b. SINTAX: a Simple Non-bayesian Taxonomy Classifier for 16S and ITS Sequences. bioRxiv.
Endo, H., Ogata, H., Suzuki, K., 2018. Contrasting biogeography and diversity patterns between diatoms and haptophytes in the central Pacific Ocean. Sci. Rep. 8, 10916.
Falkowski, P.G., Fenchel, T., Delong, E.F., 2008. The microbial engines that drive Earth's biogeochemical cycles. Science 320, 1034–1039.
Field, C.B., Behrenfeld, M.J., Randerson, J.T., Falkowski, P., 1998. Primary production of the biosphere: integrating terrestrial and oceanic components. Science 281, 237–240.
Franzè, G., Lavrentyev, P.J., 2017. Microbial food web structure and dynamics across a natural temperature gradient in a productive polar shelf system. Mar. Ecol. Prog. Ser. 569, 89–102.
Fuhrman, J.A., Steele, J.A., Hewson, I., Schwalbach, M.S., Schwalbach, M.S., Brown, M. V., Green, J.L., Brown, J.H., 2008. A latitudinal diversity gradient in planktonic marine bacteria. Proc. Natl. Acad. Sci. Unit. States Am. 105, 7774–7778.
Gaonkar, C.C., Piredda, R., Minucci, C., Mann, D.G., Montresor, M., Sarno, D., Kooistra, W.H.C.F., 2018. Annotated 18S and 28S rDNA reference sequences of taxa in the planktonic diatom family Chaetocerotaceae. PLoS One 13, e0208929.
Gaonkar, C.C., Piredda, R., Sarno, D., Zingone, A., Montresor, M., Kooistra, W.H.C.F., 2020. Species detection and delineation in the marine planktonic diatoms *Chaetoceros* and *Bacteriastrum* through metabarcoding: making biological sense of haplotype diversity. Environ. Microbiol. 22, 1917–1929.
Genitsaris, S., Monchy, S., Viscogliosi, E., Sime-Ngando, T., Ferreira, S., Christaki, U., 2015. Seasonal variations of marine protist community structure based on taxon-specific traits using the eastern English Channel as a model coastal system. FEMS Microbiol. Ecol. 91 fiv034.
Giner, C.R., Pernice, M.C., Balagué, V., Duarte, C.M., Gasol, J.M., Logares, R., Massana, R., 2020. Marked changes in diversity and relative activity of picoeukaryotes with depth in the world ocean. ISME J. 14, 437–449.
Gradinger, R., 1999. Vertical fine structure of the biomass and composition of algal communities in Arctic pack ice. Mar. Biol. 133, 745–754.
Greenblum, S., Turnbaugh, P.J., Borenstein, E., 2012. Metagenomic systems biology of the human gut microbiome reveals topological shifts associated with obesity and inflammatory bowel disease. Proc. Natl. Acad. Sci. U.S.A. 109, 594–599.
Gregory, A., Zayed, A., Conceicao-Neto, N., Temperton, B., Bolduc, B., Alberti, A., Ardyna, M., Arkhipova, K., Carmicheal, M., Cruaud, C., et al., 2019. Marine DNA viral macro-and micro-diversity from pole to pole. Cell 177, 1109–1123.
Gu, B., Wang, Y., Xu, J., Jiao, N., Xu, D., 2021. Water mass shapes the distribution patterns of planktonic ciliates (Alveolata, Ciliophora) in the subtropical Pearl River Estuary. Mar. Pollut. Bull. 167, 112341.
Guillou, L., Bachar, D., Audic, S., Bass, D., Berney, C., Bittner, L., et al., 2012. The Protist Ribosomal Reference database (PR2): a catalog of unicellular eukaryote Small Sub-Unit rRNA sequences with curated taxonomy. Nucleic Acids Res. 41, D597–D604.
Harrell, F., 2008. Hmisc: Harrell Miscellaneous. URL http://cran rproject org/web/packages/Hmisc/index html.
Hansen, P.J., Hjorth, M., 2002. Growth and grazing responses of *Chrysochromulina ericina* (Prymnesiophyceae): the role of irradiance, prey concentration and pH. Mar. Biol. 141, 975–983.
Hillebrand, H., 2004. On the generality of the latitudinal diversity gradient. Am. Nat. 163, 192–211.
Hu, S.K., Campbell, V., Connell, P., Gellene, A.G., Liu, Z., Terrado, R., Caron, D.A., 2016. Protistan diversity and activity inferred from RNA and DNA at a coastal site in the eastern North Pacific. FEMS Microbiol. Ecol. 92, fiw050.
Huang, H., Yang, J., Huang, S., Gu, B., Wang, Y., Wang, L., Jiao, N., Xu, D., 2021. Spatial distribution of planktonic ciliates in the western Pacific Ocean: along the transect from Shenzhen (China) to Pohnpei (Micronesia). Mar. Life Sci. Technol. 3, 103–115.
Hunt, G.L., Drinkwater, K.F., Arrigo, K., Berge, J., Daly, K.L., Danielson, S., et al., 2016. Advection in polar and sub-polar environments: impacts on high latitude marine ecosystems. Prog. Oceanogr. 149, 40–81.
Hutchins, D.A., Fu, F., 2017. Microorganisms and ocean global change. Nat. Microbiol. 2, 17058.
Ibarbalz, F.M., Henry, N., Brandão, M.C., Martini, S., Busseni, G., Byrne, H., Coelho, L.P., Endo, H., et al., 2019. Global trends in marine plankton diversity across kingdoms of life. Cell 179, 1084–1097.e21.
Jiang, Y., Yang, E.-J., Min, J.-O., Kim, T., Kang, S.-H., 2015. Vertical variation of pelagic ciliate communities in the western Arctic Ocean. Deep-Sea Res. Part II 120, 103–113.
Johnson, M.D., Beaudoin, D.J., 2019. The genetic diversity of plastids associated with mixotrophic oligotrich ciliates. Limnol. Oceanogr. 64, 2187–2201.
Josephson, K.L., Gerba, C.P., Pepper, I.L., 1993. Polymerase chain reaction detection of nonviable bacterial pathogens. Appl. Environ. Microbiol. 59, 3513–3515.
Ju, F., Xia, Y., Guo, F., Wang, Z., Zhang, T., 2014. Taxonomic relatedness shapes bacterial assembly in activated sludge of globally distributed wastewater treatment plants. Environ. Microbiol. 16, 2421–2432.
Kalenitchenko, D., Joli, N., Potvin, M., Tremblay, J.-É., Lovejoy, C., 2019. Biodiversity and species change in the Arctic Ocean: a view through the lens of nares strait. Front. Mar. Sci. 6, 479.
Karl, D.M., Bailiff, M.D., 1989. The measurement and distribution of dissolved nucleic acids in aquatic environments. Limnol. Oceanogr. 34, 543–558.
Katsuki, K., Takahashi, K., Onodera, J., Jordan, R.W., Suto, I., 2009. Living diatoms in the vicinity of the North Pole, summer 2004. Micropaleontology 55, 137–170.
Ladau, J., Sharpton, T.J., Finucane, M.M., Jospin, G., Kembel, S.W., O'dwyer, J., Koeppel, A.F., Green, J.L., Pollard, K.S., 2013. Global marine bacterial diversity peaks at high latitudes in winter. ISME J. 7, 1669–1677.
Legendre, P., Legendre, L., 1998. Numerical Ecology. Elsevier, Amsterdam, The Netherlands.
Levinsen, H., Nielsen, T.G., 2002. The trophic role of marine pelagic ciliates and heterotrophic dinoflagellates in arctic and temperate coastal ecosystems: a cross-latitude comparison. Limnol. Oceanogr. 47, 427–439.
Li, R., Hu, C., Wang, J., Sun, J., Wang, Y., Jiao, N., Xu, D., 2021. Biogeographical distribution and community assembly of active protistan assemblages along an estuary to a basin transect of the northern South China Sea. Microorganisms 9, 351.
Li, R., Jiao, N., Warren, A., Xu, D., 2018. Changes in community structure of active protistan assemblages from the lower pearl river to coastal waters of the South China Sea. Eur. J. Protistol. 63, 72–82.
Lima-Mendez, G., Faust, K., Henry, N., et al., 2015. Determinants of community structure in the global plankton interactome. Science 348, 1262073.
Liu, H., Probert, I., Uitz, J., Claustre, H., Aris-Brosou, S., Frada, M., Not, F., de Vargas, C., 2009. Extreme diversity in noncalcifying haptophytes explains a major pigment paradox in open oceans. Proc. Natl. Acad. Sci. U.S.A. 106, 12803–12808.
Liu, Q., Zhao, Q., McMinn, A., Yang, E.J., Jiang, Y., 2021. Planktonic microbial eukaryotes in polar surface waters: recent advances in high-throughput sequencing. Mar. Life Sci. Technol. 3, 94–102.
Logares, R., Audic, S., Bass, D., Bittner, L., Boutte, C., Christen, R., et al., 2014. Patterns of rare and abundant marine microeukaryotes. Curr. Biol. 24, 813–821.
López-García, P., Rodríguez-Valera, F., Pedrós-Alió, C., Moreira, D., 2001. Unexpected diversity of small eukaryotes in deep-sea Antarctic plankton. Nature 409, 603–607.
Lovejoy, C., Legendre, L., Price, N.M., 2002. Prolonged diatom blooms and microbial food web dynamics: experimental results from an Arctic polynya. Aquat. Microb. Ecol. 29, 267–278.
Lovejoy, C., Massana, R., Pedros-Alió, C., 2006. Diversity and distribution of marine microeukaryotes in the Arctic Ocean and adjacent seas. Appl. Environ. Microbiol. 72, 3085–3095.
Lovejoy, C., Potvin, M., 2011. Microbial eukaryotic distribution in a dynamic beaufort sea and the Arctic Ocean. J. Plankton Res. 33, 431–444.
Lubbers, G.W., Gieskes, W.W.C., del Castilho, P., Salomons, W., Bril, J., 1990. Manganese accumulation in the high pH microenvironment of *Phaeocystis* sp. (Haptophyceae) colonies from the North Sea. Mar. Ecol. Prog. Ser. 59, 285–293.
Ma, B., Wang, H.Z., Dsouza, M., Lou, J., He, Y., Dai, Z.M., et al., 2016. Geographic patterns of co-occurrence network topological features for soil microbiota at continental scale in eastern China. ISME J. 10, 1891–1901.
Magoc, T., Salzberg, S.L., 2011. FLASH: fast length adjustment of short reads to improve genome assemblies. Bioinformatics 27, 2957–2963.
Marchant, H.J., Thomsen, H.A., 1994. Haptophytes in polar waters. Systematics Association Special. In: Green, J.C., Leadbeater, B.S.C. (Eds.), The Haptophyte Algae, vol. 51. Clarenon Press, Oxford, pp. 209–228, 1994.
Marquardt, M., Vader, A., Stübner, E.I., Reigstad, M., Gabrielsen, T.M., 2016. Strong seasonality of marine microbial eukaryotes in a high-Arctic fjord (Isfjorden, in West Spitsbergen, Norway). Appl. Environ. Microbiol. 82, 1868–1880.
Massana, R., Castresana, J., Balagué, V., Guillou, L., Romari, K., Groisillier, A., et al., 2004. Phylogenetic and ecological analysis of novel marine stramenopiles. Appl. Environ. Microbiol. 70, 3528–3534.
Massana, R., Gobet, A., Audic, S., Bass, D., Bittner, L., Boutte, C., et al., 2015. Marine protist diversity in European coastal waters and sediments as revealed by high-throughput sequencing. Environ. Microbiol. 17, 4035–4049.
Matsuno, K., Yamaguchi, A., Shimada, K., Imai, I., 2012. Horizontal distribution of calanoid copepods in the western Arctic Ocean during the summer of 2008. Pol. Sci. 6, 105–119.
Mikhailov, I.S., Zakharova, Y.R., Bukin, Y.S., Galachyants, Y.P., Petrova, D.P., Sakirko, M.V., Likhoshway, Y.V., 2019. Co-occurrence networks among bacteria and microeukaryotes of Lake Baikal during a spring phytoplankton bloom. Microb. Ecol. 77, 96–109.
Milici, M., Tomasch, J., Wos-Oxley, M.L., Wang, H., Jáuregui, R., Camarinha-Silva, A., Deng, Z.L., Plumeier, I., Giebel, H.A., Wurst, M., Pieper, D.H., Simon, M., Wagner-Döbler, I., 2016. Low diversity of planktonic bacteria in the tropical ocean. Sci. Rep. 6, 19054.
Mittelbach, G.G., Schemske, D.W., Cornell, H.V., et al., 2010. Evolution and the latitudinal diversity gradient: speciation, extinction and biogeography. Ecol. Lett. 10, 315–331.
Monier, A., Terrado, R., Thaler, M., Comeau, A., Medrinal, E., Lovejoy, C., 2013. Upper Arctic Ocean water masses harbor distinct communities of heterotrophic flagellates. Biogeosciences 10, 4273–4286.
Montagnes, D.J.S., Lynn, D.H., 1991. Taxonomy of choreotrichs, the major marine planktonic ciliates, with emphasis on the aloricate forms. Mar. Microb. Food Webs 5, 59–74.
Moss, J.A., Henriksso, N.L., Pakulski, J.D., Snyder, R.A., Jeffrey, W.H., 2020. Oceanic microplankton do not adhere to the latitudinal diversity gradient. Microb. Ecol. 79, 511–515.
Not, F., del Campo, J., Balagué, V., de Vargas, C., Massana, R., 2009. New insights into the diversity of marine picoeukaryotes. PLoS One 4, e7143.
Olli, K., Wassmann, P., Reigstad, M., Ratkova, T.N., Arashkevich, E., Pasternak, A., Matrai, P.A., Knulst, J., Tranvik, L., Klais, R., Jacobsen, A., 2007. The fate of production in the central Arctic Ocean – top-down regulation by zooplankton expatriates? Prog. Oceanogr. 72, 84–113.
Onda, D.F.L., Medrinal, E., Comeau, A.M., Thaler, M., Babin, M., Lovejoy, C., 2017. Seasonal and interannual changes in ciliate and dinoflagellate species assemblages in the Arctic Ocean (amundsen gulf, beaufort sea, Canada). Front. Mar. Sci. 4, 16.
Pachauri, R.K., Allen, M.R., Barros, V.R., Broome, J., Cramer, W., Christ, R., Church, J.A., Clarke, L., Dahe, Q., Dasgupta, P., et al., 2014. Climate change 2014: synthesis report. In: Pachauri, R.K., Meyer, L. (Eds.), Contribution of Working Groups I, II and III to the Fifth Assessment Report of the Intergovernmental Panel on Climate Change. IPCC), p. 151.

Pomeroy, L.R., Williams, P.J.I., Azam, F., Hobbie, J.E., 2007. The microbial loop. Oceanography 20, 28–33.
Putt, M., 1990. Abundance, chlorophyll content and photosynthesis rates of ciliates in the Nordic Seas during summer. Deep Sea Res. 37, 1713–1731.
R Core Team, 2015. R: A Language and Environment for Statistical Computing. R Foundation for Statistical Computing, Vienna, Austria. https://www.R-project.org/.
Righetti, D., Vogt, M., Gruber, N., Psomas, A., Zimmermann, N.E., 2019. Global pattern of phytoplankton diversity driven by temperature and environmental variability. Sci. Adv. 5, eaau6253.
Salazar, G., Cornejo-Castillo, F.M., Borrull, E., Díez-Vives, C., Lara, E., Vaqué, D., Arrieta, J.M., Duarte, C.M., Gasol, J.M., Acinas, S.G., 2015. Particle-association lifestyle is a phylogenetically conserved trait in bathypelagic prokaryotes. Mol. Ecol. 24, 5692–5706.
Santoferrara, L.F., Grattepanche, J., Katz, L., McManus, G.B., 2016. Patterns and processes in microbial biogeography: do molecules and morphologies give the same answers? ISME J. 10, 1779–1790.
Schloss, P.D., Westcott, S.L., Ryabin, T., Hall, J.R., Hartmann, M., Hollister, E.B., Lesniewski, R.A., Oakley, B.B., Parks, D.H., Robinson, C.J., et al., 2009. Introducing mothur: open-source, platform-independent, community-supported software for describing and comparing microbial communities. Appl. Environ. Microbiol. 75, 7537–7541.
Schneider, L.K., Anestis, K., Mansour, J., Anschütz, A.A., Gypens, N., Hansen, P.J., John, U., Klemm, K., Martin, J.L., Medic, N., Not, F., Stolte, W., 2020. A dataset on trophic modes of aquatic protists. Biodivers. Data J. 8, e56648.
Schnepf, E., Kuhn, S.F., 2000. Food uptake and fine structure of *Cryothecomonas longipes* sp. nov., a marine nanoflagellate incertae sedis feeding phagotrophically on large diatoms. Helgol. Mar. Res. 54, 18–32.
Screen, J.A., Simmonds, I., 2010. The central role of diminishing sea ice in recent Arctic temperature amplification. Nature 464, 1334–1337.
Sherr, E.B., Sherr, B.F., Ross, C., 2013. Microzooplankton grazing impact in the Bering Sea during spring sea ice conditions. Deep-Sea Res. Pt. II 94, 57–67.
Sherr, E.B., Sherr, B.F., Wheeler, P.A., Thompson, K., 2003. Temporal and spatial variation in stocks of autotrophic and heterotrophic microbes in the upper water column of the central Arctic Ocean. Deep-Sea Res. Pt. I (50), 557–571.
Simon, N., Cras, A.L., Foulon, E., Lemée, R., 2009. Diversity and evolution of marine phytoplankton. C. R. Biol. 332, 159–170.
Sournia, A., Chrdtiennot-Dinet, M.J., Ricard, M., 1991. Marine phytoplankton: how many species in the world ocean? J. Plankton Res. 13, 1093–1099.
Stecher, A., Neuhaus, S., Lange, B., Frickenhaus, S., Beszteri, B., Kroth, P.G., Valentin, K., 2016. rRNA and rDNA based assessment of sea ice protist biodiversity from the central Arctic Ocean. Eur. J. Phycol. 51, 131–146.
Stegen, J.C., Lin, X., Fredrickson, J.K., Chen, X., Kennedy, D.W., Murray, C.J., Rockhold, M.L., Konopka, A., 2013. Quantifying community assembly processes and identifying features that impose them. ISME J. 7, 2069–2079.
Stoeck, T., Bass, D., Nebel, M., Christen, R., Jones, M.D.M., Breiner, H.W., Richards, T.A., 2010. Multiple marker parallel tag environmental DNA sequencing reveals a highly complex eukaryotic community in marine anoxic water. Microb. Ecol. 19, 21–31.
Stocker, T., et al., 2013. Climate Change 2013: the Physical Science Basis. Contribution of Working Group I to the Fifth Assessment Report of the Intergovernmental Panel on Climate Change. Cambridge University Press, Cambridge, United Kingdom and New York.
Stoeck, T., Taylor, G.T., Epstein, S.S., 2003. Novel eukaryotes from the permanently anoxic cariaco basin (caribbean sea). Appl. Environ. Microbiol. 69, 5656–5663.
Stoeck, T., Zuendorf, A., Breiner, H.-W., Behnke, A., 2007. A molecular approach to identify active microbes in environmental eukaryote clone libraries. Microb. Ecol. 53, 328–339.
Stoecker, D.K., Weigel, A.C., Stockwell, D.A., Lomas, M.W., 2014. Microzooplankton: abundance, biomass and contribution to chlorophyll in the Eastern Bering Sea in summer. Deep Sea Res. II 109, 134–144.
Stoecker, D.K., Lavrentyev, P.J., 2018. Mixotrophic plankton in the polar seas: a pan-Arctic review. Front. Mar. Sci. 5, 292.
Sun, P., Huang, L., Xu, D., Warren, A., Huang, B., Wang, Y., Wang, L., Xiao, W., Kong, J., 2019. Integrated space-time dataset reveals high diversity and distinct community structure of ciliates in mesopelagic waters of the northern South China Sea. Front. Microbiol. 10, 2178.
Sun, P., Liao, Y., Wang, Y., Yang, E.-J., Jiao, N., Lee, Y., Jung, J., Cho, K.-H., Moon, J.-K., Xu, D., 2022. Contrasting community composition and co-occurrence relationships of the active pico-sized haptophytes in the surface and subsurface chlorophyll maximum layers of the Arctic Ocean in summer. Microorganisms 10, 248.
Sun, P., Wang, Y., Laws, E., Huang, B., 2020. Water mass-driven spatial effects and environmental heterogeneity shape microeukaryote biogeography in a subtropical, hydrographically complex ocean system - a case study of ciliates. Sci. Total Environ. 706, 135753.
Sun, P., Zhang, S., Wang, Y., Huang, B., 2021. Biogeographic role of the Kuroshio Current intrusion in the microzooplankton community in the boundary zone of the northern South China Sea. Microorganisms 9, 1104.
Terrado, R., Medrinal, E., Dasilva, C., Thaler, M., Vincent, W.F., Lovejoy, C., 2011. Protist community composition during spring in an Arctic flaw lead polynya. Polar Biol. 34, 1901–1914.
Thaler, M., Lovejoy, C., 2014. Environmental selection of marine stramenopile clades in the Arctic Ocean and coastal waters. Polar Biol. 37, 347–357.
Thomas, M.K., Kremer, C.T., Klausmeier, C.A., Litchman, E., 2012. A global pattern of thermal adaptation in marine phytoplankton. Science 338, 1085–1088.
Tillmann, U., Hesse, K.J., Tillmann, A., 1999. Large-scale parasitic infection of diatoms in the northfrisian wadden sea. J. Sea Res. 42, 255–261.
Toseland, A., Daines, S.J., Clark, J.R., Kirkham, A., Strauss, J., Uhlig, C., Lenton, T.M., Valentin, K., Pearson, G.A., Moulton, V., Mock, T., 2013. The impact of temperature on marine phytoplankton resource allocation and metabolism. Nat. Clim. Change 3, 979.
Unrein, F., Gasol, J.M., Not, F., Forn, I., Massana, R., 2014. Mixotrophic haptophytes are key bacterial grazers in oligotrophic coastal waters. ISME J. 8, 164–176.
Vaquer-Sunyer, R., Duarte, C.M., Holding, J., Regaudie-de-Gioux, A., García-Corral, L.S., Reigstad, M., Wass- mann, P., 2013. Seasonal patterns in arctic planktonic metabolism (fram strait – svalbard region). Biogeosciences 10, 1451–1469.
Vernet, M., 1991. Phytoplankton dynamics in the Barents Sea estimated from chlorophyll budget models. Polar Res. 10, 129–145.
Willig, M.R., Kaufman, D.M., Stevens, R.D., 2003. Latitudinal gradients of biodiversity: pattern, process, scale, and synthesis. Annu. Rev. Ecol. Evol. Syst. 34, 273–309.
Woodd-Walker, R.S., Ward, P., Clarke, A., 2002. Large-scale patterns in diversity and community structure of surface water copepods from the Atlantic Ocean. Mar. Ecol. Prog. Ser. 236, 189–203.
Xia, X., Cheung, S., Endo, H., Suzuki, K., Liu, H., 2019. Latitudinal and vertical variation of *synechococcus* assemblage composition along 170° W transect from the south pacific to the Arctic Ocean. Microb. Ecol. 77, 333–342.
Xu, D., Kong, H., Yang, E.-J., Li, X., Jiao, N., Warren, A., Wang, Y., Lee, Y., Jung, J., Kang, S.-H., 2020. Contrasting community composition of active microeukaryotes in melt ponds and sea water of the Arctic Ocean revealed by high throughput sequencing. Front. Microbiol. 11, 1170.
Xu, D., Li, R., Hu, C., Sun, P., Jiao, N., Warren, A., 2017. Microeukaryote diversity and activity in the water column of the South China Sea based on DNA and RNA high throughput sequencing. Front. Microbiol. 8, 1121.
Xu, D., Sun, P., Zhang, Y., Li, R., Huang, B., Jiao, N., Warren, A., Wang, L., 2018a. Pigmented microeukaryotes fuel the deep sea carbon pool in the tropical Western Pacific Ocean. Environ. Microbiol. 20, 3811–3824.
Xu, G., Yang, E., Jiang, Y., Cho, K., Jung, J., Lee, Y., Kang, S., 2018b. Can pelagic ciliates indicate vertical variation in the water quality status of western Arctic pelagic ecosystems? Mar. Pollut. Bull. 133, 182–190.
Yang, J., Huang, S., Fan, W., Warren, A., Jiao, N., Xu, D., 2020. Spatial distribution patterns of planktonic ciliate communities in the East China Sea: potential indicators of water masses. Mar. Pollut. Bull. 156, 111253.
Zhao, F., Wang, Y., Zheng, S., Zhao, R., Lin, M., Xu, K., 2021. Patterns and drivers of microeukaryotic distribution along the north equatorial current from the central Pacific Ocean to the south China sea. Mar. Pollut. Bull. 165, 112091.
Zheng, S., Wang, G., Zhang, F., Cai, M., He, J., 2011. Dominant diatom species in the Canada Basin in summer 2003, a reported serious melting season. Polar Rec. 47, 244–261.